



# Enhanced NO<sub>2</sub> gas sensing of a single-layer MoS<sub>2</sub> by photogating and piezo-phototronic effects

Junmeng Guo<sup>a,b,1</sup>, Rongmei Wen<sup>a,b,1</sup>, Junyi Zhai<sup>a,b,c,\*</sup>, Zhong Lin Wang<sup>a,b,d,\*</sup>

<sup>a</sup>CAS Center for Excellence in Nanoscience, Beijing Institute of Nanoenergy and Nanosystems, Chinese Academy of Sciences, Beijing 100083, China

<sup>b</sup>School of Nanoscience and Technology, University of Chinese Academy of Sciences, Beijing 100049, China

<sup>c</sup>Center on Nanoenergy Research, School of Physical Science and Technology, Guangxi University, Nanning 530004, China

<sup>d</sup>School of Materials Science and Engineering, Georgia Institute of Technology, Atlanta, GA 30332, USA

## ARTICLE INFO

### Article history:

Received 24 October 2018

Received in revised form 12 November 2018

Accepted 30 November 2018

Available online 07 December 2018

### Keywords:

Ultrahigh sensitivity  
Flexible NO<sub>2</sub> sensor  
Single-layer MoS<sub>2</sub>  
Photogating effect  
Piezo-phototronic effect

## ABSTRACT

NO<sub>2</sub> sensors with ultrahigh sensitivity are demanded for future electronic sensing systems. However, traditional sensors are considerably limited by the relative low sensitivity, high cost and complicated process. Here, we report a simply and reliable flexible NO<sub>2</sub> sensor based on single-layer MoS<sub>2</sub>. The flexible sensor exhibits high sensitivity to NO<sub>2</sub> gas due to ultra-large specific surface area and the nature of two-dimensional (2D) semiconductor. When the NO<sub>2</sub> is 400 ppb (parts per billion), compared with the dark and strain-free conditions, the sensitivity of the single-layer sensor is enhanced to 671% with a 625 nm red light-emitting diode (LED) illumination of 4 mW/cm<sup>2</sup> power under 0.67% tensile strain. More important, the response time is dramatically reduced to ~16 s and it only needs ~65 s to complete 90% recovery. A theoretical model is proposed to discuss the microscopic mechanisms. We find that the remarkable sensing characteristics are the result of coupling among piezoelectricity, photoelectricity and adsorption-desorption induced charges transfer in the single-layer MoS<sub>2</sub> Schottky junction based device. Our work opens up the way to further enhancements in the sensitivity of gas sensor based on single-layer MoS<sub>2</sub> by introducing photogating and piezo-phototronic effects in mesoscopic systems.

© 2018 Science China Press. Published by Elsevier B.V. and Science China Press. All rights reserved.

## 1. Introduction

NO<sub>2</sub>, a poisonous gas, has been considered as a key index for vehicle emissions, industrial waste gas and environmental monitoring [1–3]. The development of simple, low-cost and high-efficiency sensors to trace NO<sub>2</sub> gas is vitally desirable. In the previous work, numerous nanomaterials have been widely investigated for NO<sub>2</sub> detection, such as carbon nanotubes [4,5] and metal oxide of specific structures (e.g., ZnO nanorods, TiO<sub>2</sub> nanotubes, Cu<sub>2</sub>O nanoparticles) [6–9]. They have shown high sensitivity to NO<sub>2</sub> gas sensing. Compared with these traditional sensors built on a hard substrate, the flexible sensor has a broad application prospect for the future market. Two-dimensional (2D) graphene is a fascinating material for gas sensing due to ultra-large specific surface area, remarkable flexibility and easy integration [10–12]. However, the pristine graphene exhibits bad sensing behavior to NO<sub>2</sub> gas [13,14] due to the poor interaction between gas molecules and

the lattice atoms. Although surface modulated or functionalized graphene shows higher sensitivity and selectivity than that of the pristine graphene [15–17], these cumbersome methods are often regarded as time-consuming, high-cost and poor controllability. Moreover, it remains challenging for these decorative graphene sensors to detect the parts per billion (ppb) level gas rapidly and precisely at room temperature due to the semi-metal nature. Especially, the zero band gap of graphene further restricts the application on the electronics and optoelectronics sensors [18–20]. Up to now, it is still difficult to open up a optimal band gap perfectly and precisely in graphene because of the complicated process and limited technological capability. Fortunately, the emergence of graphene-like 2D semiconducting materials has successfully bypassed the complicated problem from another point of view, and brings the chance to fulfill the long-cherished wish.

As an important member of semiconductor transition metal dichalcogenides (TMDCs) family, single-layer 2D molybdenum disulfide (MoS<sub>2</sub>) exhibits remarkable physical properties, such as unique electronic and optoelectronic properties [21], stunning mechanical flexibility [22], ideal interfacial van der Waals (vdw) interaction [23] and ultra-large surface-to-volume ratio [24]. These

\* Corresponding authors.

E-mail addresses: [jyzhai@binn.cas.cn](mailto:jyzhai@binn.cas.cn) (J. Zhai), [zhong.wang@mse.gatech.edu](mailto:zhong.wang@mse.gatech.edu) (Z. L. Wang).

<sup>1</sup> These authors contributed equally to this work.

properties endow a preponderant position to sense NO<sub>2</sub> gas over thicker ones, one-dimensional (1D) or bulk semiconductor materials. Recently, 2D MoS<sub>2</sub> based field effect transistor (FET) sensor draw researchers' interest because of ultra-high response to gas molecule [25,26]. However, these traditional individual bare FET sensors often require a large external gate bias to achieve high sensitivity [27,28]. Especially, to the atomically thin 2D semiconductor materials, the extremely big gate bias is also at the expense of lifetime and power consumption, which have inevitable drawback to potential application. More importantly, the response and recovery time is still slow to practical application even under a high gate bias [29]. Therefore, searching other means to further enhance the detection performance of single-layer MoS<sub>2</sub> based gas sensor is urgently needed. The piezotronic effect is observed in asymmetric crystal structures materials, e.g., wurtzite-structure semiconductor materials [30–32]. When there is an external mechanical stimulus to the device, the piezoelectric polarization charges (piezocharges) or piezoelectric potential (piezopotential) is produced along the polar direction, which can modulate the carrier transport at the metal-semiconductor junction area. Besides, the strain-induced piezocharges/piezopotential can also effectively tune the generation, separation and recombination of photoexcited electron-hole pairs at the metal-semiconductor/hetero-junction, which is the piezo-phototronic effect [33–35]. Interestingly, the single-layer MoS<sub>2</sub> has presented in-plane ultimate atomic-scale piezotronic and piezo-phototronic properties owing to the non-central symmetric crystal structure [36,37].

In this work, we demonstrate the enhanced sensing behavior of single-layer MoS<sub>2</sub> Schottky junction based NO<sub>2</sub> sensors by introducing photogating and piezo-phototronic effects instead of traditional gate bias modulation. The results suggest that the sensitivity of the single-layer sensor can be enhanced by tuning the Schottky barrier height (SBH) utilizing the photogating and piezo-phototronic effects. Furthermore, the response (recovery) time has been drastically reduced to dozens of seconds due to the direct band gap ultrathin MoS<sub>2</sub> Schottky contacts under photo-excitation, which is much better than previous reports [29,38]. We believe that the flexible single-layer MoS<sub>2</sub> based sensor is quite promising for future miniaturization, portable and ultra-sensitive gas sensing systems.

## 2. Materials and methods

### 2.1. The monolayer MoS<sub>2</sub> film synthesis

Monolayer MoS<sub>2</sub> thin films were deposited on a 300 nm SiO<sub>2</sub>/Si substrate by carrying out chemical vapor deposition (CVD). MoO<sub>3</sub> powder (13 mg, 99.95%) was added to a quartz boat, and cleaned ultrasonically SiO<sub>2</sub>/Si substrate was placed face down in the boat. Then, the quartz boat was put in the middle zone of the furnace. Solid sulfur (350 mg, 99.95%, Sigma Aldrich) was placed upstream from the middle zone of the furnace. The whole length between MoO<sub>3</sub> powder and solid sulfur was about 20 cm. In order to remove the air, the furnace was first pump down to 0 Pa. Then, the furnace temperature was increased to 800 °C in 15 °C/min with 20 sccm (standard cubic centimeter per minute) argon gas. Meanwhile, when the furnace temperature was increased to 600 °C, the S-zone temperature was ramped up to about 210 °C quickly by the heating tape. After 30 min deposition, the sample was quickly cooled down to room temperature under 100 sccm Ar gas.

### 2.2. Material characterization and transfer

The deposited MoS<sub>2</sub> thin film by CVD was characterized using photoluminescence (PL) and Raman spectroscopy (100 × objective

with laser spot size of ~1 μm, 532 nm excitation laser, Renishaw Raman). The single-layer MoS<sub>2</sub> film was transferred onto a polyethylene terephthalate (PET) substrate, and Cr/Pd/Au (1 nm/20 nm/50 nm) electrodes were patterned parallel to the zigzag direction via the previous methods [41].

### 2.3. Photogating and piezo-phototronic effects on a single-layer MoS<sub>2</sub> gas sensor

Piezotronic effect of single-layer MoS<sub>2</sub> based sensor was performed by using a Keithley 4200 semiconductor characterization system to record the electrical characteristics in a home-made closed cavity. The whole test was carried out in a dark environment. During the optical testing, the light intensity was recorded by a Controlled Intensity Modulated system (IT6834 ITECH DC Power Supply) under a 625 nm red monochromatic light-emitting diode (LED) illumination. For the sensing examination, the 30 ppm Ar-diluted NO<sub>2</sub> gas were mixed with pure Ar to achieve a certain concentrations before being injected into the chamber. The concentrations of the NO<sub>2</sub> gas were controlled by a flow gate switch which were recorded by a built-in gas concentration detector.

## 3. Result and discussion

For gas sensors, recently, most reports have demonstrated that the Schottky contact performs higher sensitivity and faster response speed than the Ohmic contact [39,40]. The Schottky barrier at the metal/semiconductor interface plays a crucial role in tuning the electrical transport of the metal-semiconductor-metal (M-S-M) structure. It is generally recognized that the change of the SBH can magnifies the influence of the gas molecules adsorbed at the junction area. Although a lot of progress has been made in enhanced gas sensing by the modulation of piezotronic effect on the SBH [41,42], very limited research has been conducted on the localized and quantitatively controlled coupling of photogating and piezo-phototronic effect on the gas sensing field. Here, we design an atomically thin Schottky-contacted sensor using two back-to-back Pd-MoS<sub>2</sub> junctions on the flexible and PET substrate for NO<sub>2</sub> detection. MoS<sub>2</sub> triangles were grown on the SiO<sub>2</sub>/Si substrate by CVD at 850 °C for 30 min. Fig. 1a shows that the side-lengths of these equilateral triangles are about 10–30 μm. As shown in Fig. S1 (online), the atomic force microscopy (AFM) image shows the step height of the MoS<sub>2</sub> triangle is about 0.72 nm. The observed Raman spectrum of a MoS<sub>2</sub> triangle consists of two peaks at 385.5 cm<sup>-1</sup> (in plane mode E<sub>2g</sub><sup>1</sup>) and 405.5 cm<sup>-1</sup> (out-of-plane mode A<sub>1g</sub><sup>1</sup>), respectively, and the gap between the two peaks is 20 cm<sup>-1</sup> (Fig. 1b). Thus, the ultrathin triangle MoS<sub>2</sub> is single-layer [43]. The PL measurement was performed using a 532 nm laser. Fig. 1c shows that the single-layer MoS<sub>2</sub> triangle is a direct gap semiconductor, which consists of two peaks at 620 and 670 nm. In order to fabricate flexible NO<sub>2</sub> gas sensor, MoS<sub>2</sub> monolayers were first perfectly transferred onto a flexible PET substrate, where did not cause defects and contamination. The previous research noted that the zigzag (in spite of “Mo” or “S”) is the dominant morphologies of CVD triangles, and the relevance to this morphology allows us to easily identify the armchair “X” and zigzag “Y” orientation with the triangle edge terminations of CVD grown MoS<sub>2</sub> by optical microscopy [44]. Since the highest in-plane piezoelectric response has been observed when strain is applied along the “X” direction of the single-layer MoS<sub>2</sub> crystal [45], two metal electrodes made of Cr/Pd/Au (1 nm/20 nm/40 nm) were then deposited on the MoS<sub>2</sub> surface paralleled to “Y” orientation. Fig. 1d shows a typical flexible gas sensor with a single-layer MoS<sub>2</sub> triangle outlined by black dashed line. When the flexible PET

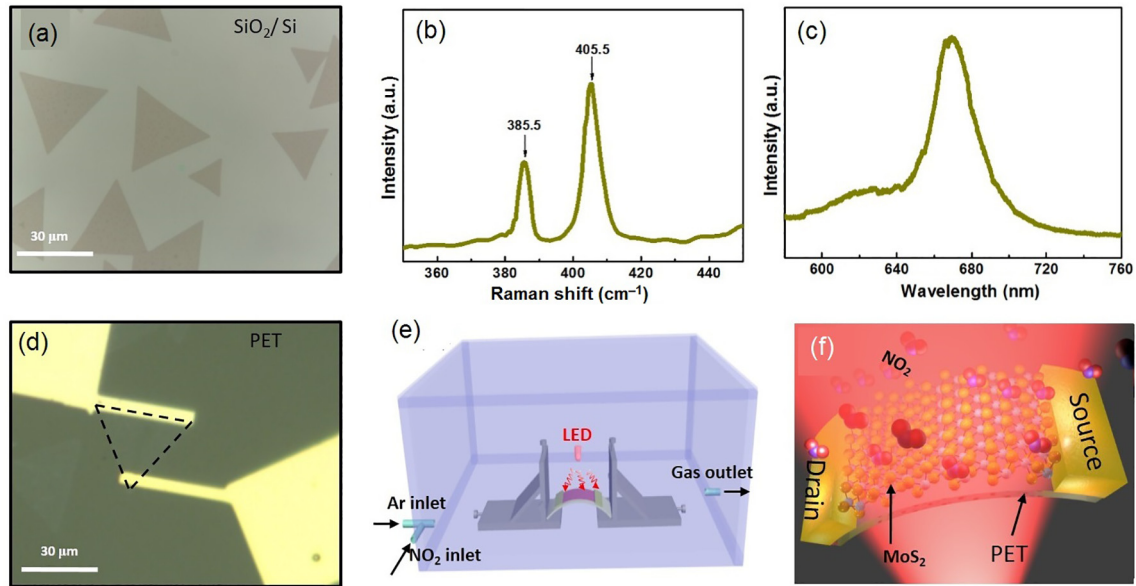


**Fig. 1.** (Color online) Single-layer MoS<sub>2</sub> gas sensor. (a) Optical microscopy image of the as-grown MoS<sub>2</sub> monolayer on a SiO<sub>2</sub>/Si substrate. (b) Raman spectrum of a single-layer MoS<sub>2</sub> flake. (c) PL spectrum of a single-layer MoS<sub>2</sub> flake. (d) A flexible two-terminal single atomic layer MoS<sub>2</sub> gas sensor transferred onto PET flexible substrate. (e) Schematic of the measurement set-ups for studying the piezo-phototronic effect in a single-layer MoS<sub>2</sub> based NO<sub>2</sub> sensor. (f) Schematic of a flexible single-layer MoS<sub>2</sub> based NO<sub>2</sub> gas sensing device.

substrate is bended upward, the MoS<sub>2</sub> flake experienced a static tensile strain accordingly. Therefore, we could systematically study the enhanced sensing behavior of the 2D sensor to NO<sub>2</sub> gas detection by photogating and piezo-phototronic effects. In this work, the maximum strain is controlled at 0.7% to avoid the sample slippage and electrode crack. All measurements of the as-fabricated Schottky-contacted single-layer MoS<sub>2</sub> based sensor were performed at room temperature.

For our gas sensor, the M-S-M contact can be equivalent to two back-to-back Schottky barrier structures, and the reversely bias Pd-MoS<sub>2</sub> Schottky barrier primarily control the carriers transport when there is a bias voltage applied [46]. Fig. 1e shows the schematic of the measurement set-ups, and Fig. 1f shows schematic of the flexible single-layer MoS<sub>2</sub> based NO<sub>2</sub> gas sensing device. First, the single-layer MoS<sub>2</sub> device was placed in the sealed chamber under dark environment, and the current sensing response of this single-layer sensor was investigated by recording the current change when the chamber environment changed from pure argon gas (Ar) to a certain concentration of NO<sub>2</sub>. The measured *I-V* curves in Fig. 2a display nonlinear and rectification behavior. The current rectifying properties is caused by the Schottky barriers formed between the metal Pd electrodes and the semiconductor in the single-layer MoS<sub>2</sub> device, and the shape of the *I-V* curve depends on the heights of the Schottky barriers formed at the drain and source sides due to the difference of the effective contact areas and interface/surface states [35,47]. For the single-layer MoS<sub>2</sub> gas sensor, changes in the semiconducting behaviors with strain may arise from the piezoresistance effect or the piezotronic effect. The piezoresistive effect is a symmetrical effect on the electrical transport properties that has the same effect on contact at both sides [48,49] and can not induce charge polarization. Unlike the piezoresistive effect, the piezotronic effect is asymmetrical change in electrical characteristics, which is the strain-induced polarization charges to modulate the heights of the metal-semiconductor Schottky barrier [50]. As shown in Fig. 2a, the asymmetrical change of *I-V* characteristics in both the forward and the reverse directions by adjusting the strain should be caused by the piezotronic effect rather than the piezoresistive effect. Under both 20 ppb NO<sub>2</sub> and

dark conditions, the current increases from 0.24 to 0.93 nA (by 387%) with increasing the tensile strain from 0 to 0.67% when a positive bias voltage of 10 V is applied. As shown in Fig. S2 (online), similar enhancements are observed at other NO<sub>2</sub> concentrations by increasing the tensile strain. When a 0.31% strain is applied (Fig. 2b), the output signals drops at both sides as NO<sub>2</sub> gas is stepwise introduced. Similar responses are observed for other strain conditions (Fig. S3 online), which are mainly attributed to the decreased carrier concentration caused by charge transfer and the increased SBH at the M-S junction area. The whole trend of current response of the flexible sensor to different strains and various NO<sub>2</sub> concentrations can be seen clearly in Fig. S4 (online).

The sensitivity is defined in Supplementary data (online). As shown in Fig. 2c, taking the sensor at 400 ppb NO<sub>2</sub> concentration as an example, compared with strain-free condition, the sensor shows a highest sensitivity of 499% when 0.67% strain is applied. Similar phenomenon has also been observed at other NO<sub>2</sub> concentrations. In particular, the change of sensitivity stepwise increases as the strain increases from 0 to 0.67%, which indicates an excellent modulation in SBH by piezotronic effect. The change of SBH at the drain side ( $\Delta\phi_d$ ) is quantitatively extracted by the classic thermionic emission-diffusion theory (Supplementary data, online). As shown in Fig. S5 (online), compared with strain-free condition, the sensor shows a highest  $\Delta\phi_d$  of -33.49 meV under 20 ppb NO<sub>2</sub> concentration when 0.67% strain is applied. Similar calculations are presented for other NO<sub>2</sub> concentrations, which is consist with the enhancement of sensitivity before. Thus, once a static tensile strain is applied, the strain-induced positive polarization charges at the drain side can effectively reduce the barrier height at the local Schottky junction. Finally, the more free electronics drift in the space charge region, the more NO<sub>2</sub> is adsorpted thus enhancing the sensitivity of the gas sensor.

Recently, photogating instead of tradition gate bias shows great application prospect in promoting sensitivity and response/recovery time of Schottky-contacted semiconducting based oxidizing gas sensors at room temperature [51–53]. Herein, we furthest improve the sensitivity to trace NO<sub>2</sub> gas with a single-layer MoS<sub>2</sub> based sensor by photogating and piezo-phototronic effect. *I-V*

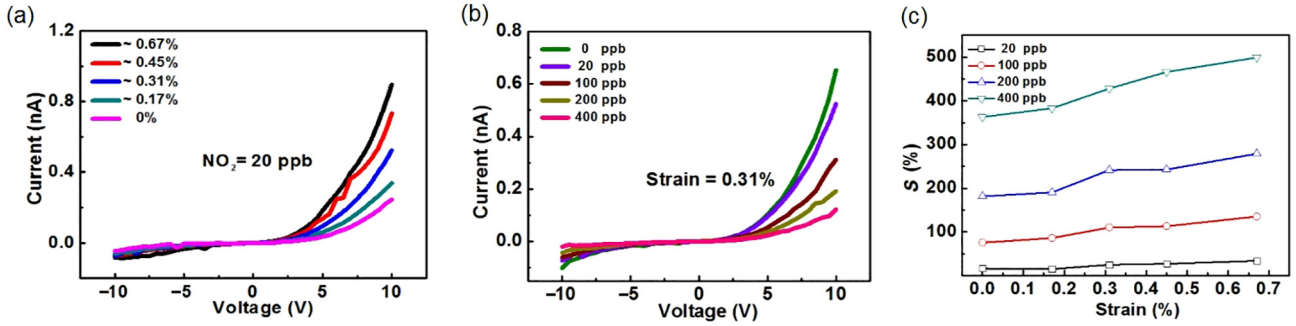


**Fig. 2.** (Color online)  $\text{NO}_2$  concentration dependence of the piezotronic effect on the single-layer  $\text{MoS}_2$  device is summarized. The  $I$ - $V$  curves of the gas sensor under (a) 20 ppb  $\text{NO}_2$  concentration, and (b) 0.31% strain. (c) The sensitivity ( $S$ ) of the gas sensor to different tensile strains with changing  $\text{NO}_2$  concentration from 20 to 400 ppb.

characteristics of the sensor are measured by applying strain under various illumination intensities and  $\text{NO}_2$  concentrations. When the 20 ppb  $\text{NO}_2$  gas is introduced into the sealed chamber, the current of this device under both 10 V bias voltages and strain-free conditions increases from 0.25 nA in dark to 10.38 nA with  $9 \text{ mW/cm}^2$  illumination intensity (Fig. 3a). When 0.67% strain is applied, the current increases from 0.9 nA in dark to 73.03 nA with  $9 \text{ mW/cm}^2$  illumination intensity (Fig. S6 online). Similar phenomenons are observed at other  $\text{NO}_2$  concentrations by increasing the tensile strain and light illumination intensity (Fig. 3b). The results suggest that the current under certain  $\text{NO}_2$  concentration stepwise increases with increasing of either the strain or

illumination intensity. Therefore, the trend of current output improves significantly by photogating and piezo-phototronic effect.

For this kind of sensor, there are two reasons to explain the enhanced behavior by light illumination. On one hand, when the light is illuminated over the sensor, the incident photon induces fermi-level lift in semiconductor materials, leading to producing electron-hole pairs, and then photogenerated electrons leap into the conduction band, which can be collected at the Schottky junction area by the applied external field. As a result, the output signal is enhanced. On the other hand, the photogenerated electrons within the conduction band can also be effectively trapped by the oxidizing gas molecule, leading to the current decline.

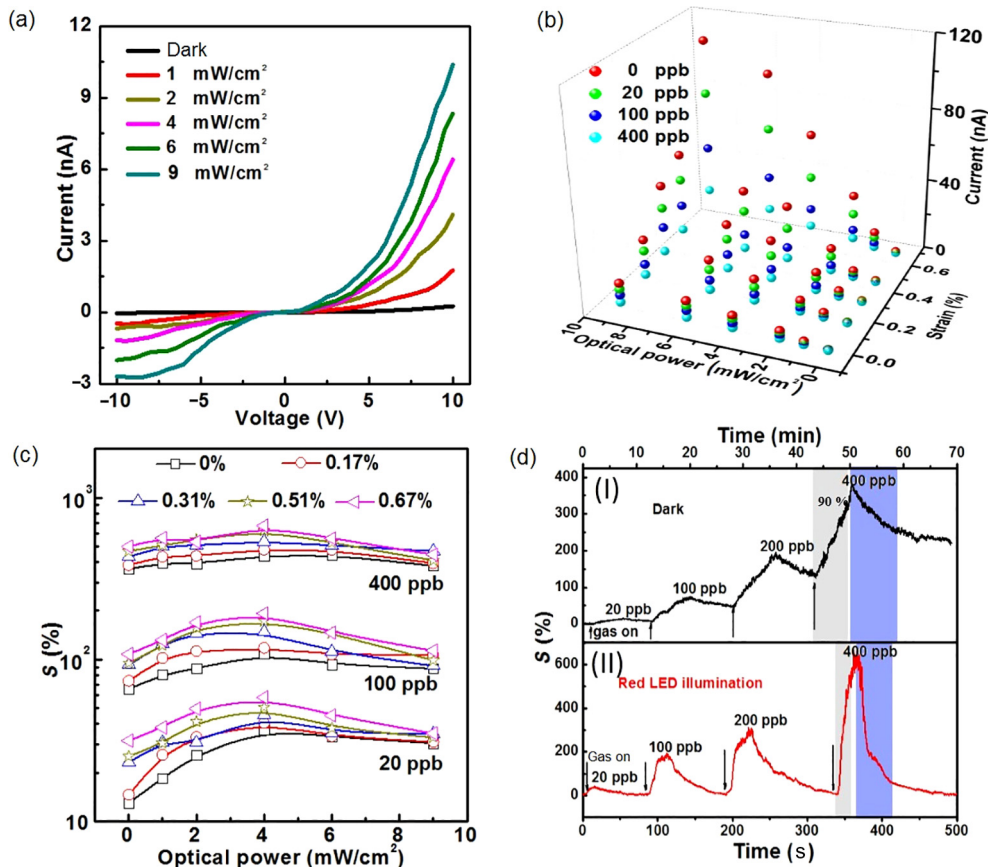


**Fig. 3.** (Color online) Piezo-phototronic effects in single-layer  $\text{MoS}_2$  based  $\text{NO}_2$  sensor. (a) The  $I$ - $V$  curves of the gas sensor under 20 ppb  $\text{NO}_2$  concentration and strain-free conditions. (b) Three-dimensional (3D) graph depicting the current response of the  $\text{NO}_2$  sensor under different strains, gas concentrations and light intensities at a bias voltage of 10 V. (c) The sensitivity of the sensor under different strains, gas concentrations and light intensities at a bias voltage of 10 V. (d) The response and recovery time of the  $\text{NO}_2$  sensor under (I) both dark and strain-free conditions; (II) both  $4 \text{ mW/cm}^2$  red LED illumination and 0.67% tensile strain conditions.

Accordingly, the modulation of the sensitivity is mainly determined by the dynamic balance between the two competitive processes, the photo-induced electrons emergence and adsorption-desorption induced charges transfer. For noncentrosymmetric semiconductors, the strain-induced polarization charges at the M-S contact can well modulate the photocurrent. For instance, it can effectively affect the separation, recombination and transport processes of carriers in the vicinity of the contacts, which can be due to the piezo-phototronic effect.

In order to intuitively observe the modulation of the flexible NO<sub>2</sub> sensor by the photogating and piezo-phototronic effect, the sensitivity of this NO<sub>2</sub> sensor under various strains and illumination intensities is calculated in Fig. 3c. These results clearly show that, under strain-free and a certain NO<sub>2</sub> concentration, the sensitivity increase first and then decrease with the increase of light intensity. In this sensor, the phenomenon can be understood as follows: first, with the light illuminates the single-layer MoS<sub>2</sub> sensor, the photo-induced electron-hole pairs produced in the conduction and valence bands [ $h\nu \rightarrow e^- + h^+$ ]. When the light intensity is lower than 4 mW/cm<sup>2</sup>, the photo-excited electrons adsorption rate to NO<sub>2</sub> gas is much higher than the holes desorption rate. The possible reason is that lots of existing NO<sub>2</sub> in the surrounding of the sensor are more conducive to adsorption and prevent desorption. In other word, the electrons adsorption to NO<sub>2</sub> gas [NO<sub>2</sub>(g) + e<sup>-</sup> → NO<sub>2</sub><sup>-</sup>(ad)] is in dominant in this case, leading to increasing the sensitivity of the sensor. When the light intensity is higher than 4 mW/cm<sup>2</sup>, the remarkable rise holes drift in the valence band, resulting in an improvement of the gas desorption rate [NO<sub>2</sub><sup>-</sup>(ad) + h<sup>+</sup> → NO<sub>2</sub>(g)]. Meanwhile, the electrons adsorption to NO<sub>2</sub> gas in the conduction band will reach saturation in a suitable light intensity because not all electrons get to react with NO<sub>2</sub> gas. Therefore, the sensitivity of the sensor decreases with further increasing of the light intensity. The optimal value is determined by the NO<sub>2</sub> adsorption/deposition ratio. Furthermore, at a certain NO<sub>2</sub> concentration and light intensity, the sensitivity increases with increasing of the strain. Taking the sensor at 400 ppb NO<sub>2</sub> concentrations and 4 mW/cm<sup>2</sup> as an example, the sensitivity increases from 436% to 670% as the strain increases from 0 to 0.67%. Similar phenomenon has also been observed at other NO<sub>2</sub> concentrations and light intensities. The result shows that the strain-induced polarization charges at both sides can largely affect the sensitivity of the sensor. When the light intensity is higher than 4 mW/cm<sup>2</sup>, we can also observed that the enhanced performance of sensitivity by piezotronic effect gradually become weak with further increasing the light intensity, which can be understood by the truth that the more free carriers can more effectively screen the piezoelectric polarization charges at the junction area as compared to the case at lower light

intensity. Obviously, the modulations by the photogating and piezo-phototronic effect to various concentrations of NO<sub>2</sub> are distinguishing. This experimental phenomenon should, in principle, be attributed to the competition among piezoelectricity, photoelectricity and adsorption-deposition induced charges transfer in the single-layer MoS<sub>2</sub> device. Nevertheless, the detection sensitivity of the NO<sub>2</sub> sensor is furthest enhanced by photogating and piezo-phototronic effect.

To examine the NO<sub>2</sub>-sensing behavior of the single-layer MoS<sub>2</sub> based piezo-phototronic sensor, the response time and recovery time measurements are carried out at four different concentrations of NO<sub>2</sub> ranging from 20 to 400 ppb. Under both dark and strain-free conditions (in Fig. 3d(I)), it takes ~8 min to reach saturation to various NO<sub>2</sub> concentrations, and more than ~20 min to attain less than half recovery of the original state. In fact, the sensor often need a few hours to achieve full recovery, which is also correspond with the previous report of MoS<sub>2</sub> sensor on hard SiO<sub>2</sub>/Si substrate [29]. This phenomenon demonstrates that the process of the flexible NO<sub>2</sub>-sensing is still reversible though the recovery time is lengthy. When applied both light (4 mW/cm<sup>2</sup> illumination) and strain (0.67%) to the flexible sensor, the response time has been dramatically reduced to ~16 s. More importantly, the full recovery time decreased to ~65 s from a few hours (Fig. 3d(II)). We also found that the sensitivity still remains largely stability after many repeated measurements for the flexible sensor. Obviously, compared to other NO<sub>2</sub> gas sensor (Table 1), the photogating and piezo-phototronic activated flexible single-layer MoS<sub>2</sub> sensor manifesting high sensitivity and much quicker response/recovery behavior. The high sensitivity and rapid sensing characteristic should be due to the photo-activated free carriers transfer and piezocharges-induced Schottky barrier modulation.

The physical mechanism of the enhancement behavior of single-layer MoS<sub>2</sub> based NO<sub>2</sub> sensor by photogating and piezo-phototronic effects can be understood by the band diagram in Fig. 4. Under both dark and strain-free conditions, as shown in Fig. 4a, the two back-to-back Schottky contacts between the single-layer MoS<sub>2</sub> and the Pd electrodes have distinctly different barrier heights ( $\phi_s > \phi_d$ ). The current of drain side is higher than that of source side because the reversely biased Schottky barrier mainly control the free electrons transport, and present rectification behavior. By introducing the NO<sub>2</sub> gas into the chamber, the NO<sub>2</sub> gas is adsorbed on the surface of the single-layer MoS<sub>2</sub>, and forms an electron depletion region, which leads to the charges transfer from conductor band to acceptor. Moreover, the negative charges around the vicinity of Schottky-contacted Pd-MoS<sub>2</sub> interface will increase the SBH at both junctions [39]. Thus, the current of reverse-biased Schottky diode decreases at both sides with

**Table 1**  
Summary of sensing performance of different NO<sub>2</sub> sensors.

| Substrate            | Methods     | Materials                     | T (°C) | Detection limit (ppm) | [Formula]    | Sensitivity (%) | Response/recovery time | Reference |
|----------------------|-------------|-------------------------------|--------|-----------------------|--------------|-----------------|------------------------|-----------|
| Flexible PET         | CVD         | GO (multilayer)               | RT     | 5                     | $\Delta R/R$ | 40              | 30 min/>30 min         | [10]      |
| Flexible paper       | CVD         | GO (monolayer)                | RT     | 200                   | $\Delta R/R$ | 39              | 180 s/>1000 s          | [11]      |
| Flexible PET         | CVD         | rGO                           | RT     | 20                    | $\Delta R/R$ | 25              | >700 s/1500 s          | [17]      |
| Flexible PET         | LBL-SA      | MWCNT                         | RT     | 15                    | $\Delta R/R$ | 1,910           | >700 s/>1100 s         | [4]       |
| Flexible PI/PET      | Chemical    | WO <sub>3</sub> -MWCNTs-rGO   | RT     | 5                     | $\Delta R/R$ | 1,400           | 7 min/15 min           | [5]       |
| Glass                | Evaporation | ZnO                           | 200    | 100                   | $\Delta R/R$ | 722             | 35 s/26 s              | [6]       |
| Glass                | CSP         | Ni-ZnO                        | 200    | 100                   | $\Delta R/R$ | 115             | 11 s/>123 s            | [8]       |
| Ceramic              | Chemical    | Cu <sub>2</sub> O             | 50     | 50                    | $R_g/R$      | 710             | 20 s/131 s             | [9]       |
| Ti                   | Chemical    | Cr-TiO <sub>2</sub>           | 500    | 100                   | $R_g/R$      | 350             | 15 min/15 min          | [7]       |
| SiO <sub>2</sub> /Si | CVD         | MoS <sub>2</sub> (monolayer)  | RT     | 0.4                   | $\Delta G/G$ | 80              | 8 min/>12 min          | [29]      |
| SiO <sub>2</sub> /Si | Exfoliating | MoS <sub>2</sub> (5 layer)    | RT     | 100                   | $\Delta R/R$ | 200             | 7 min/>15 min          | [27]      |
| SiO <sub>2</sub> /Si | CVD         | MoS <sub>2</sub> (multilayer) | RT     | 100                   | $\Delta R/R$ | 33              | 29 s/350 s             | [54]      |
| Flexible PET         | CVD         | MoS <sub>2</sub> (monolayer)  | RT     | 0.4                   | $\Delta R/R$ | 670             | 16 s/65 s              | This work |

$R_g$ : the resistance of the device in NO<sub>2</sub> gas;  $R$ : the resistance of the device in dry N<sub>2</sub> or Ar;  $G_g$ : the conductance of the device in NO<sub>2</sub> gas;  $G$ : the conductance of the device in dry N<sub>2</sub> or Ar;  $\Delta R = R_g - R$ ,  $\Delta G = G_g - G$ .

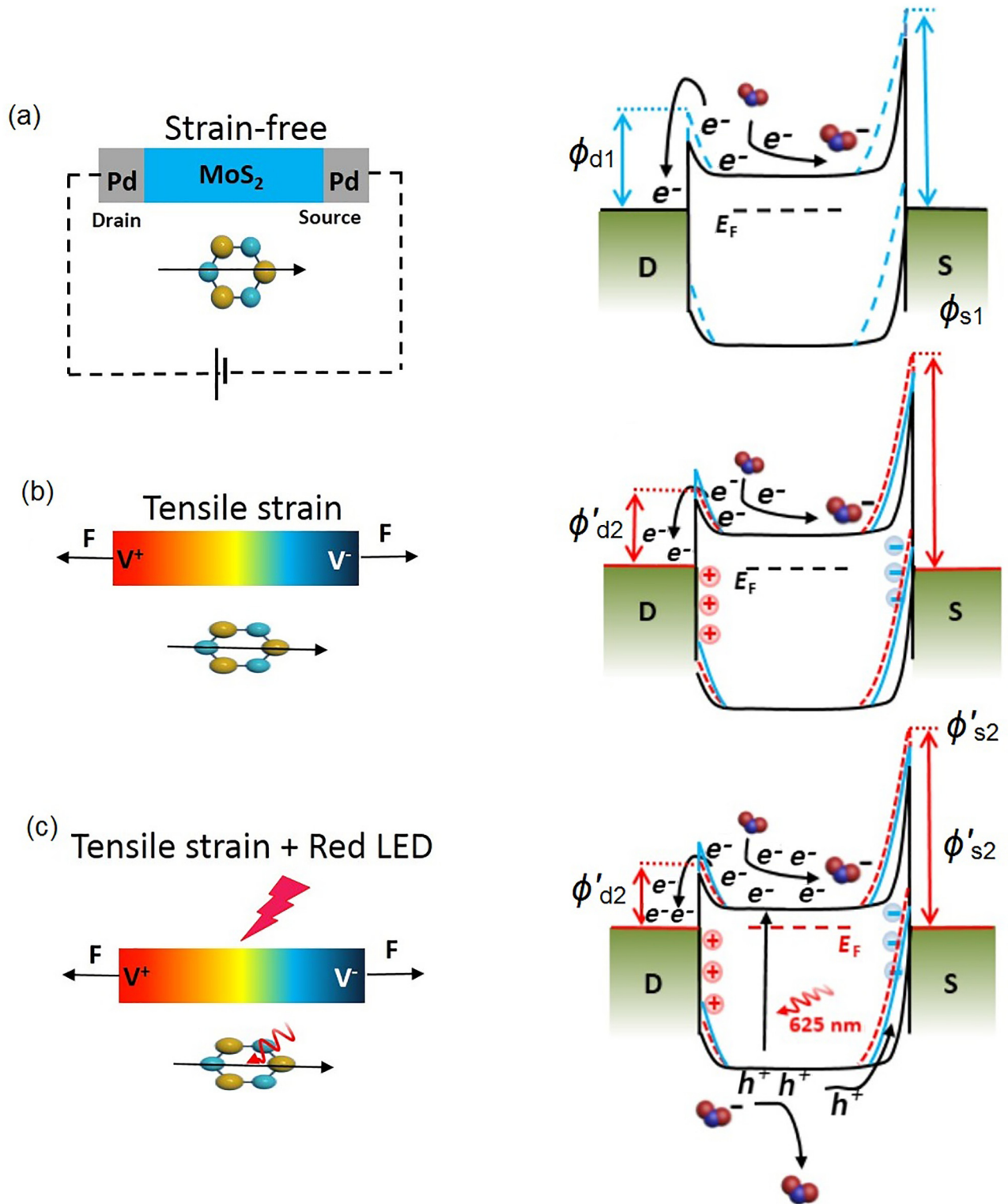


**Fig. 4.** (Color online) Schematic energy band diagram illustrating the asymmetric Schottky barriers at the source and drain sides. (a) The pristine single-layer MoS<sub>2</sub> based NO<sub>2</sub> sensor under a strain-free condition and dark environment. (b) The piezotronic-tuned single-layer MoS<sub>2</sub> based NO<sub>2</sub> sensor under a certain NO<sub>2</sub> atmosphere. (c) The piezotronic-tuned single-layer MoS<sub>2</sub> based NO<sub>2</sub> sensor under both a certain NO<sub>2</sub> atmosphere and a red LED illumination.

introducing the NO<sub>2</sub> gas. For the N-type semiconductor, the number of holes at the space charge region is almost zero in the dark environment. When we stop flowing the NO<sub>2</sub> gas, there is no hole to participate in the gas desorption process, resulting in the full recovery spending as long as a few hours. When a tensile strain

is applied (Fig. 4b), due to the non-central symmetric crystal structure of single-layer MoS<sub>2</sub>, the polarization charges appeared near the Schottky junctions. The positive polarization charges at the drain side pull down the barrier height at the Schottky junction. Thus, with a positive bias, the more free electronics drift in the

space charge region, which leads to the more NO<sub>2</sub> adsorbed. Finally, the sensitivity of the gas sensor is further enhanced. When the appropriate light and strain were introduced to the flexible sensor (Fig. 4c), the photo-excited electrons accelerate the NO<sub>2</sub> gas adsorption, leading to a dramatic improvement of the sensitivity. Meanwhile, the strain-induced electrical polarization appeared near the Schottky contacts because of the asymmetric crystal structure in atomically thin MoS<sub>2</sub>. The positive piezocharges at the drain side reduce the SBH, indicating that the more free carriers drift in the space charge region at a positive bias. Finally, the sensitivity and response time of the NO<sub>2</sub> sensor is further enhanced because more adsorption emerges at the junction area of the device. When we stop flowing the NO<sub>2</sub> gas, the NO<sub>2</sub> concentration in the sealed cavity decreases to zero quickly. In this case, the adsorption/desorption balance is broken, and result in that the desorption process dominated by the holes plays a major role than adsorption caused by electronics. Thus, the dramatic acceleration of recovery ultimately should be due to the Schottky barrier modulation by photogating and piezo-phototronic effect.

#### 4. Conclusion

In conclusion, we have fabricated a flexible NO<sub>2</sub> sensor based on single-layer MoS<sub>2</sub>. The strain-induced piezocharges can effectively control the electronics and optoelectronics transportation by tuning the SBH. The results suggest that the sensitivity and sensing performance of the single-layer MoS<sub>2</sub> based sensor for NO<sub>2</sub> detection can be dramatically enhanced by applying tensile strains and light illuminations. For example, under 400 ppb NO<sub>2</sub>, compared with the dark and strain-free conduction, the sensitivity of the single-layer sensor is enhanced 671% with a 625 nm red LED illumination of 4 mW/cm<sup>2</sup> power under a tensile strain of 0.67%. More importantly, the response time is dramatically reduced from ~6 min to ~16 s and it only takes ~65 s to complete 90% recovery. In fact, the sensitivity modulation of the flexible NO<sub>2</sub> sensor is the result of the coupling among piezoelectricity, photoelectricity and surface charges transfer in the direct band gap ultrathin MoS<sub>2</sub> Schottky contacts. This work has practical importance for developing future gas sensor at low cost and high performance.

#### Conflict of interest

The authors declare that they have no conflict of interest.

#### Acknowledgments

This work was supported by the National Key Research and Development Program of China (2016YFA0202703, 2016YFA0202704), the National Natural Science Foundation of China (51472056), the Thousands Talents Plan For Pioneer Researcher And His Innovation Team, China, and the Recruitment Program of Global Youth Experts, China.

#### Appendix A. Supplementary data

Supplementary data to this article can be found online at <https://doi.org/10.1016/j.scib.2018.12.009>.

#### References

- [1] Ji SL, Wang HB, Yan DH, et al. A high-performance room-temperature NO<sub>2</sub> sensor based on an ultrathin heterojunction film. *Adv Mater* 2013;25:1755–60.
- [2] Hoffmann MWG, Prades J, Mayrhofer L, et al. Highly selective SAM-nanowire hybrid NO<sub>2</sub> sensor: insight into charge transfer dynamics and alignment of frontier molecular orbitals. *Adv Funct Mater* 2014;24:595–602.

- [3] Jalil AR, Chang H, Schmidt OG, et al. Fully integrated organic nanocrystal diode as high performance room temperature NO<sub>2</sub> sensor. *Adv Mater* 2016;28:2971–7.
- [4] Su PG, Lee CT, Chuang YS, et al. Fabrication of flexible NO<sub>2</sub> sensors by layer-by-layer self-assembly of multi-walled carbon nanotubes and their gas sensing properties. *Sens Actuators B Chem* 2009;139:488–93.
- [5] Yaqoob U, Iftekhhar ASM, Chung GSA. High-performance flexible NO<sub>2</sub> sensor based on WO<sub>3</sub> NPs decorated on MWCNTs and RGO hybrids on PI/PET substrates. *Sens Actuators B Chem* 2016;224:738–46.
- [6] Navalea YH, Navaleb ST, Patila VB, et al. Zinc oxide hierarchical nanostructures as potential NO<sub>2</sub> sensors. *Sens Actuators B Chem* 2017;251:551–63.
- [7] Gönüllü Y, Haidry AA, Saruhan B. Nanotubular Cr-doped TiO<sub>2</sub> for use as high-temperature NO<sub>2</sub> gas sensor. *Sens Actuators B Chem* 2015;217:78–87.
- [8] Ganbavle VV, Inamdar SI, Rajpure KY, et al. Synthesis of fast response highly sensitive and selective Ni:ZnO based NO<sub>2</sub> sensor. *Chem Eng J* 2016;286:36–7.
- [9] Wang L, Zhang R, Zhang T, et al. Concave Cu<sub>2</sub>O octahedral nanoparticles as an advanced sensing material for benzene (C<sub>6</sub>H<sub>6</sub>) and nitrogen dioxide (NO<sub>2</sub>) detection. *Sens Actuators B Chem* 2016;223:311–7.
- [10] Choi HK, Jeong HY, Cho SY, et al. Flexible NO<sub>2</sub> gas sensor using multilayer graphene films by chemical vapor deposition. *Carbon Lett* 2013;14:186–9.
- [11] Yang G, Lee C, Pearson SJ, et al. Flexible graphene-based chemical sensors on paper substrates. *PCCP* 2013;15:1798–801.
- [12] Li W, Kong L, Chen C, et al. Experimental realization of honeycomb borophene. *Sci Bull* 2018;63:282–6.
- [13] Pearce R, Iakimov T, Yakimova R, et al. Epitaxially grown graphene based gas sensors for ultra sensitive NO<sub>2</sub> detection. *Sens Actuators B Chem* 2011;155:451–5.
- [14] Ko G, Kim HY, Kim J, et al. Graphene-based nitrogen dioxide gas sensors. *Curr Appl Phys* 2010;10:1002–4.
- [15] Chung MG, Kim DH, Kim YH, et al. Highly sensitive NO<sub>2</sub> gas sensor based on ozone treated grapheme. *Sens Actuators B Chem* 2012;166:172–6.
- [16] Su PG, Shieh HC. Flexible NO<sub>2</sub> sensors fabricated by layer-by-layer covalent anchoring and in situ reduction of graphene oxide. *Sens Actuators B Chem* 2014;190:865–72.
- [17] Wu J, Tao K, Norford LK, et al. Improved selectivity and sensitivity of gas sensing using a 3D reduced graphene oxide hydrogel with an integrated microheater. *ACS Appl Mater Interfaces* 2015;7:27502–10.
- [18] Balog R, Jørgensen B, Sljivancanin Z, et al. Bandgap opening in graphene induced by patterned hydrogen adsorption. *Nat Mater* 2010;9:315–9.
- [19] Dong Y, Wu ZS, Ren W, et al. Graphene: a promising 2D material for electrochemical energy storage. *Sci Bull* 2017;62:724–40.
- [20] Bonaccorso F, Sun Z, Ferrari AC. Graphene photonics and optoelectronics. *Nat Photon* 2010;4:611–22.
- [21] Yuan J, Chen W, Lou J. Two dimensional heterostructure: perfect platform for exploring interface interaction. *Sci Bull* 2017;62:381–2.
- [22] Zhang K, Zhai J, Wang ZL, et al. A flexible p-CuO/n-MoS<sub>2</sub> heterojunction photodetector with enhanced photoresponse by the piezo-phototronic effect. *Mater Horiz* 2017;4:274–80.
- [23] Aiyiti A, Bai X, Wu J, et al. Measuring the thermal conductivity and interfacial thermal resistance of suspended MoS<sub>2</sub> using electron beam self-heating technique. *Sci Bull* 2018;63:452–8.
- [24] Lv D, Wang H, Zhu D, et al. Atomic process of oxidative etching in monolayer molybdenum disulfide. *Sci Bull* 2017;62:846–51.
- [25] Li H, Yin Z, Zhang H, et al. Fabrication of single- and multilayer MoS<sub>2</sub> film-based field-effect transistors for sensing NO at room temperature. *Small* 2012;8:63–7.
- [26] He Q, Zeng Z, Zhang H, et al. Fabrication of flexible MoS<sub>2</sub> thin-film transistor arrays for practical gas-sensing applications. *Small* 2012;8:2994–9.
- [27] Late DJ, Huang YK, Rao CNR, et al. Sensing behavior of atomically thin-layered MoS<sub>2</sub> transistors. *ACS Nano* 2013;7:4879–91.
- [28] Zhao J, Li N, Zhang GY, et al. Highly sensitive MoS<sub>2</sub> humidity sensors array for noncontact sensation. *Adv Mater* 2017;29:1702076.
- [29] Liu B, Chen L, Zhou C, et al. High-performance chemical sensing using Schottky-contacted chemical vapor deposition grown monolayer MoS<sub>2</sub> transistors. *ACS Nano* 2014;8:5304–14.
- [30] Chen L, Xue F, Wang ZL, et al. Strain-gated field effect transistor of a MoS<sub>2</sub>-ZnO 2D–1D hybrid structure. *ACS Nano* 2015;10:1546–51.
- [31] Wang ZL. Piezopotential gated nanowire devices: piezotronics and piezo-phototronics. *Nano Today* 2010;5:540–52.
- [32] Peng M, Zhang Y, Wang ZL, et al. Magnetic-mechanical-electrical-optical coupling effects in GaN-based LED/rare-earth Terfenol-D structures. *Adv Mater* 2014;26:6767–72.
- [33] Wang ZL. Progress in piezotronics and piezo-phototronics. *Adv Mater* 2012;24:4632–46.
- [34] Liu CH, Peng M, Zhai J, et al. Interface engineering on p-CuI/n-ZnO heterojunction for enhancing piezoelectric and piezo-phototronic performance. *Nano Energy* 2016;26:417–24.
- [35] Zhou J, Gu Y, Fei P, et al. Flexible piezotronic strain sensor. *Nano Lett* 2008;8:3035–40.
- [36] Wu W, Wang L, Wang ZL, et al. Piezoelectricity of single-atomic-layer MoS<sub>2</sub> for energy conversion and piezotronics. *Nature* 2014;514:470–4.
- [37] Wu W, Wang L, Wang ZL, et al. Piezophototronic effect in single-atomic-layer MoS<sub>2</sub> for strain-gated flexible optoelectronics. *Adv Mater* 2016;28:8463–648.
- [38] Zhang D, Liu Z, Zhou C, et al. Detection of NO<sub>2</sub> down to ppb Levels using Individual and multiple In<sub>2</sub>O<sub>3</sub> nanowire devices. *Nano Lett* 2004;4:1919–24.

- [39] Wei T, Yeh P, Wang ZL, et al. Gigantic enhancement in sensitivity using schottky contacted nanowire nanosensor. *J Am Chem Soc* 2009;131:17690–5.
- [40] Hu Y, Zhou J, Wang ZL, et al. Supersensitive fast-response nanowire sensors by using schottky contacts. *Adv Mater* 2010;22:3327–32.
- [41] Guo J, Wen R, Wang ZL, et al. Piezotronic effect enhanced flexible humidity sensing of monolayer MoS<sub>2</sub>. *ACS Appl Mater Interfaces* 2018;10:8110–6.
- [42] Niu S, Hu Y, Wang ZL, et al. Enhanced performance of flexible ZnO nanowire based room-temperature oxygen sensors by piezotronic effect. *Adv Mater* 2013;25:3701–6.
- [43] Hu Z, Bao Y, Li Z, et al. Temperature dependent Raman and photoluminescence of vertical WS<sub>2</sub>/MoS<sub>2</sub> monolayer heterostructures. *Sci Bull* 2017;62:16–21.
- [44] Vander Zande AM, Huang PY, Hone J, et al. Grains and grain boundaries in highly crystalline monolayer molybdenum disulphide. *Nat Mater* 2013;12:554–61.
- [45] Zhu H, Wang Y, Zhang X, et al. Observation of piezoelectricity in free-standing monolayer MoS<sub>2</sub>. *Nat Nanotechnol* 2015;10:151–5.
- [46] Liu Y, Zhang Y, Wang ZL, et al. Fundamental theories of piezotronics and piezo-phototronics. *Nano Energy* 2015;14:257–75.
- [47] Zhang Z, Yao K, Liu Y, et al. Quantitative analysis of current-voltage characteristics of semiconducting nanowires: decoupling of contact effects. *Adv Funct Mater* 2007;17:2478–89.
- [48] Zhang Y, Yan X, Yang Y, et al. Scanning probe study on the piezotronic effect in ZnO nanomaterials and nanodevices. *Adv Mater* 2012;24:4647–55.
- [49] Zhang X, Liao Q, Liu S, et al. Poly(4-styrenesulfonate)-induced sulfur vacancy self-healing strategy for monolayer MoS<sub>2</sub> homojunction photodiode. *Nat Commun* 2017;8:15881.
- [50] Zhang Z, Liao Q, Yu Y, et al. Enhanced photoresponse of ZnO nanorods-based self-powered photodetector by piezotronic interface engineering. *Nano Energy* 2014;9:237–44.
- [51] Guo L, Yang Z, Dou X. Artificial olfactory system for trace identification of explosive vapors realized by optoelectronic schottky sensing. *Adv Mater* 2017;29:1604528.
- [52] An X, Liu F, Kar S, et al. Tunable graphene-silicon heterojunctions for ultrasensitive photodetection. *Nano Lett* 2013;13:909–16.
- [53] Li X, Zhu H, Wu D, et al. Graphene-on-silicon schottky junction solar cells. *Adv Mater* 2010;22:2743–8.
- [54] Kumar R, Goel N, Kumar M. UV-activated MoS<sub>2</sub> based fast and reversible NO<sub>2</sub> sensor at room temperature. *ACS Sens* 2017;2:1744–52.



Junyi Zhai received his Ph.D. degree from Virginia Polytechnic Institute and State University in 2009. Now he is Professor at Beijing Institute of Nanoenergy and Nanosystems, Chinese Academy of Sciences. His main research interests are micro/nano piezoelectric semiconductors, sensors and self-power systems.



Zhong Lin Wang received his Ph.D. from Arizona State University in physics. He now is the Hightower Chair in Materials Science and Engineering, Regents' Professor, Engineering Distinguished Professor and Director, Center for Nanostructure Characterization, at Georgia Tech. His research on self-powered nanosystems has inspired the worldwide effort in academia and industry for studying energy for micro-nano-systems, which is now a distinct disciplinary in energy research and future sensor networks. He coined and pioneered the field of piezotronics and piezo-phototronics by introducing piezoelectric potential gated charge transport process in fabricating new electronic and optoelectronic device.



Junmeng Guo received his Bachelor from Henan University. He is currently a Ph.D. candidate supervised by Prof. Junyi Zhai at Beijing Institute of Nanoenergy and Nanosystems, Chinese Academy of Sciences. His research interests include 2D nanomaterials fabrication and characteristics.